ÉTOILE: A Three-Dimensional Finite Element Code for Analyzing Fuel Pin Deformations in an LMFBR Assembly

M. Nakagawa
NAIG Nuclear Research Laboratory, Nippon Atomic Industry Group Co., Ltd., 4-1, Ukishima-cho, Kawasaki 210, Japan

SUMMARY

Computer program ÉTOILE has been developed for the purpose of predicting irradiation behaviour of fuel pins in a fuel subassembly under steady state conditions in LMFBR cores.

This report describes the analytical models and numerical procedures together with some typical results obtained by the code.

ÉTOILE is programmed with the FORTRAN-IV capable of treating up to 271 fuel pins in a subassembly, and up to 20 turns of spiral wires.

The finite element method is employed in the code to perform the three-dimensional structural analysis of the full bundle model. In order to represent the non-linear stiffness caused by contacts and separations between adjacent pins, a new joint element has been developed.

A model for treating the effect of wire tension is included in the code to simulate the pin and wire mechanical interaction caused by different dimensional change between the wire and the fuel cladding during irradiation.

With the finite element method for discretization of the structural equations, a set of non-linear equations is obtained. To solve the non-linear equations, an iteration technique is used. Two iteration loops are used, one is the outer iteration loop concerning the non-linearity due to wire tension, and another is the inner iteration loop concerning the non-linearity due to contact and separation. For the acceleration of inner iteration, the Newton-Raphson method is adopted. In each iteration step, the linear matrix equation, which is often the king size matrix equation, must be reconstructed and then solved. To solve the linear matrix equation, the block successive over-relaxation method is adopted.

To see the effect of wire tension, some analyses were made on the two subassemblies containing 169 and 37 fuel pins respectively. As a result, it was shown that there were significant effects of wire tension on the equilibrium configuration of fuel pins in both cases.

This work was performed under the sponsorship of Toshiba Corporation.

1. Introduction

The influences of temperature gradients, neutron fluence gradients and irradiation induced creep lead individually to different bowing behaviours effects of all fuel pins in a fuel subassembly of a fast reactor. Subsequent contacts between neighbouring fuel pins result in forces of different strength. Eventually all fuel pins will be rearranged in such a way that an equilibrium of forces between all fuel pins is achieved. The determination of this equlibrium configuration is of high significance especially from a safety point of view.

In wire-wrapped type fuel pins as shown in Fig. 1, there exist tension forces in spiral wires, which are generated in fabrication processes and by temperature difference between the fuel cladding and the spiral wire. Based on the results of the post irradiation experiments in the fast reactor Phenix, it was recently reported that these tension forces would play significant roles in forming the equilibrium configuration /1/.

In the present study, therefore, a theoretical approach, which takes account of the wire tension effect by means of the finite element method, is proposed to assess the three-dimensional equilibrium configuration of fuel pins in a fuel subassembly under steady state condition. A computer program ÉTOILE has been developed with this theoretical approach. The code is capable of treating 19 to 271 fuel pins in a fuel subassembly, and the maximum number of turns of spiral wire is 20.

In the first part of this paper, the basic model of the problem and the discretization by means of the finite element method are described. The solution algorithm of the program ÉTOILE is briefly presented in the second part. In the last part, comparisons are made between ÉTOILE resulsts obtained with and without the effects of wire tension forces.

2. Theoretical Formulation

2.1 Analytical Model

2.1.1 Geometrical Model

A fairly simple model for fuel pins is employed to achieve a reasonable computer economy. Each single circular pin is considered to be a beam. Each beam is axially subdivided into six finite elements per one wire turn as indicated in Fig. 2. This finite element is represented by a three-dimensional isoparametric element with six-degrees of freedom per each nodal point (designated by ● in Fig. 2).

A joint element is incorporated to represent the non-linear stiffness caused by contacts and separations of pins. These elements are placed between adjacent nodal points in each nodal plane where contacts between adjacent elements are most likely to occur (Fig. 3).

2.1.2 Physical Model

The beam element is assumed to consist of a homogeneous, isotropic and elastic material, and adequately described by a small-deformation theory /2/.

The joint element /3/ is defined under the following assumptions:

(1) There is no resistance against net tension in the normal direction.

(2) There is high resistance against compression.

(3) Friction effect is ignored.

The wire tension effect is considered by means of the surface integrations of the reaction forces due to wire tensions. The tension of each wire is dependent on the state of the deflections of the corresponding beam elements from normal position. Hence, an iteration technique has to be used. A simple iteration method is adopted in ÉTOILE.

2.1.3 Boundary Conditions

In a LMFBR fuel assembly, permanent cross-sectional deformation of the hexagonal duct is induced by the following two mechanisms: (1) void swelling and (2) bulging in-plane bending mode due to irradiation and thermal creep under the coolant pressure gradient across the duct wall. This deformation can be computed by means of the simplified method proposed by D. P. Chan /4/.

The mechanical equilibrium at any time step is analyzed under the following boundary conditions:

(1) The bottoms of fuel pins are fixed.

(2) The positions of the inner faces of the duct wall are fixed at the positions corresponding to the permanent deformation up to the time step.

2.2 Finite Element Procedure /5/

2.2.1 Derivation of Explicit non-linear equations.

With the principle of virtual work, the equilibrium equation, in the presence of contact non-linearities, initial strains and wire tensions, is obtained in the matrix notation as

$$\int_V \underset{\sim}{B}^T \underset{\sim}{\sigma} \, dV - \int_A \underset{\sim}{N}^T \underset{\sim}{t} \, dA = 0 \tag{1}$$

where $\underset{\sim}{B}$ is the strain shape function matrix, $\underset{\sim}{\sigma}$ the stress vector, $\underset{\sim}{N}$ the displacement shape function matrix and $\underset{\sim}{t}$ the force vector imposed on fuel pin surface due to the wire tension. The superscript T indicates the transpose of the matrix, $\int_V dV$ the integral taken over the whole volume and $\int_A dA$ over the whole surface of all fuel pins.

The displacement vector $\underset{\sim}{u}$ and the total strain vector $\underset{\sim}{\varepsilon}$ are expressed in terms of the nodal displacement vector $\underset{\sim}{r}$ as

$$\underset{\sim}{u} = \underset{\sim}{N} \underset{\sim}{r} \quad ; \quad \underset{\sim}{\varepsilon} = \underset{\sim}{L} \underset{\sim}{u} = \underset{\sim}{L} \underset{\sim}{N} \underset{\sim}{r} \equiv \underset{\sim}{B} \underset{\sim}{r} \tag{2}$$

where $\underset{\sim}{L}$ is a suitable linear operator.

The stress-strain relation for the beam elements is written as

$$\underset{\sim}{\sigma} = \underset{\sim}{D}_c \, (\underset{\sim}{\varepsilon} - \underset{\sim}{\varepsilon}_o) \tag{3}$$

where $\underset{\sim}{D}_c$ is an elasticity matrix and $\underset{\sim}{\varepsilon}_o$ is the initial strain vector summing up thermal, swelling and creep strains. A similar relation for the joint elements is approximated using differential notation as

$$d\underset{\sim}{\sigma} = \underset{\sim}{D}_J \, d\underset{\sim}{\varepsilon} \tag{4}$$

where

$$\underset{\sim}{D}_J > 0 \qquad \text{at contract state}$$
$$\underset{\sim}{D}_J = 0 \qquad \text{at separated state}$$

Let the following non-linear equation represent above equation.

$$\underset{\sim}{\sigma} = \overline{\underset{\sim}{D}}_J(\underset{\sim}{r})\ \underset{\sim}{\varepsilon} \tag{5}$$

Substitution of eq.(2), (3) and (5) into eq.(1) gives explicit non-linear equation relating total nodal displacement vector $\underset{\sim}{r}$ with total load vector $\underset{\sim}{f}(\underset{\sim}{r})$.

$$(\underset{\sim}{K}_c + \overline{\underset{\sim}{K}}_J(\underset{\sim}{r}))\underset{\sim}{r} = \underset{\sim}{f}(\underset{\sim}{r}) \tag{6}$$

where

$$\underset{\sim}{K}_c = \int_{V_c} \underset{\sim}{B}_c^T\ \underset{\sim}{D}_c\ \underset{\sim}{B}_c\ dV = \sum_{e=1}^{E_c} \int_{V_c^{(e)}} \underset{\sim}{B}_c^{(e)T}\ \underset{\sim}{D}_c^{(e)}\ \underset{\sim}{B}_c^{(e)}\ dV \tag{7}$$

$$\overline{\underset{\sim}{K}}_J(\underset{\sim}{r}) = \int_{V_J} \underset{\sim}{B}_J^T\ \overline{\underset{\sim}{D}}_J(\underset{\sim}{r})\ \underset{\sim}{B}_J\ dV$$

$$= \sum_{e=1}^{E_J} \int_{V_J^{(e)}} \underset{\sim}{B}_J^{(e)T}\ \overline{\underset{\sim}{D}}_J^{(e)}(\underset{\sim}{r})\ \underset{\sim}{B}_J^{(e)}\ dV \tag{8}$$

$$\underset{\sim}{f}(\underset{\sim}{r}) = \int_{A_c} \underset{\sim}{N}_c^T\ \underset{\sim}{t}(\underset{\sim}{r})dA + \int_{V_c} \underset{\sim}{B}_c^T\ \underset{\sim}{D}_c\ \underset{\sim}{\varepsilon}_o\ dV$$

$$= \sum_{e=1}^{E_c} \left(\int_{A_c^{(e)}} \underset{\sim}{N}_c^{(e)T}\ \underset{\sim}{t}^{(e)}(\underset{\sim}{r})\ dA + \int_{V_c^{(e)}} \underset{\sim}{B}_c^{(e)T}\ \underset{\sim}{D}_c^{(e)}\ \underset{\sim}{\varepsilon}_o^{(e)}\ dV \right) \tag{9}$$

The subscript c indicates values corresponding to the beam elements, J to the joint elements, and the superscript (e) to the finite element (e). E is the total number of the finite elements.

2.2.2 Iteration Technique

To solve the non-linear eq.(6), two iteration loops are adopted. One is the outer iteration loop concerning $\underset{\sim}{f}(\underset{\sim}{r})$ and another is the inner iteration loop concerning $(\underset{\sim}{K}_c + \overline{\underset{\sim}{K}}_J(\underset{\sim}{r}))$.

For the outer iteration, a simple iteration method is adopted, in which the nodal force vector shown by the first integral in the summation of eq.(9) is calculated repeatedly for the deformed shapes of the fuel pins in each step of outer iteration until convergence is obtained.

For the inner iteration, the Newton-Raphson method /5/ is adopted, in which a linear matrix equation representing the tangential stiffness characteristics of eq.(6) is solved repeatedly until convergence is obtained. The linear matrix equation, which is the king size matrix equation in this problem, is solved with the block successive over-relaxation method /6/.

2.3 Derivation of Stiffness Matrix

2.3.1 Beam element

For the stiffness matrix of a beam element shown by the last integral of eq.(7), a common element is adopted /7/.

2.3.2 Joint element

This section aims to derive the stiffness matrix of a joint element shown by the last integral of eq.(8).

Fig.4 shows the configuration of the adjacent fuel pins in the initial state and in the deformed state at some nodal plane. Where (y', z') and (y", z") represent the local co-ordinate. Yi and Zi indicate the positions of fuel pins in the global co-ordinate.

In addition to the previously mentioned assumptions in Section 2.1.2., the following assumption is adopted.

> If the contact occures on any plane slightly above or below a nodal plane, it is assumed that the contact occures on the corresponding nodal plane.

From this assumption, we can assume that the spiral wire is located just between the two adjacent pins (indicated by dotted circle in Fig. 4). Thus, the following criterion is obtained to judge the occurrence of contacts.

$$L_{1,2} = \sqrt{(\Delta Y_1 - \Delta Y_2)^2 + (GAP + \Delta Z_1 - \Delta Z_2)^2}$$

$$L_{1,2} \leqq R_1 + R_2 + d \qquad \text{contact state} \qquad (10)$$

$$L_{1,2} > R_1 + R_2 + d \qquad \text{separated state}$$

where GAP is the distance between O_1 and O_2 in the initial state, Ri is the radius of the fuel pin i in the deformed state and d is the diameter of the spiral wire in the deformed state.

For the deformed state, the stiffness matrix $\underset{\sim}{K}_J^{(e)''}$ in the local co-ordinate (y", z") is described as

$$\underset{\sim}{K}_J^{(e)''} = \begin{bmatrix} 0 & 0 & 0 & 0 \\ 0 & Kn & 0 & -Kn \\ 0 & 0 & 0 & 0 \\ 0 & -Kn & 0 & Kn \end{bmatrix}$$

$$Kn = K_{in} \qquad \text{at contact state}$$

$$Kn = 0 \qquad \text{at separated state} \qquad (11)$$

where Kin is the compression stiffness of a fuel pin. In the above eq., the order of the freedoms is $(v_1'', w_1'', v_2'', w_2'')$, where v_i'' is the translational displacement to the y'' axis of the nodal point i, and w_i'' to the z'' axis.

To obtain the stiffness matrix in the global co-ordinate (y, z), the transformation of the co-ordinate from (y'', z'') to (y, z) is imposed on $\underset{\sim}{K}_J^{(e)''}$. Finally, the joint stiffness matrix $\underset{\sim}{K}_J^{(e)}$ in the global co-ordinate (y,z) is obtained as

$$\underset{\sim}{K}_J^{(e)} = \begin{bmatrix} KnS^2 & KnSC & -KnS^2 & -KnSC \\ & KnC^2 & -KnSC & -KnC^2 \\ & & KnS^2 & KnSC \\ (\text{Symmetry}) & & & KnC^2 \end{bmatrix}$$

with

$$S = \sin\alpha, \qquad C = \cos\alpha \tag{12}$$

where α is the rotational angle observing from the Z'' axis to the Z axis.

For the joint element represinting the pin to duct contact, a similar equation is obtained.

3. The Program ÉTOILE

ÉTOILE code has been developed according to the mathematical method explained so far.

Fig.5 shows the block chart of ÉTOILE. In addition to the two iteration loops explained in Sec.2.2.2, the time step loop is incorporated to analyze fuel pin deformations during irradiation.

The basic input to the code is the fuel subassembly geometry, the material properties, and the temperature and nuetron flux distributions. The code has the capability of linking up with the subchannel code, such as COBRA IV /8/, through peripheral files as shown with broken lines in Fig.5.

To improve the creep relaxation calculation, the computations of creep and swelling strains are repeated at some intervals in each time-step under the assumptions that the nodal displacements are unchanged in the time step.

To save the computer time required for the iteration loop associated with contact and separation, the substructure method /5/ /9/ is adopted. In the part of the contact & separation loop in Fig.5, the freedoms of the translational and rotational displacement of x-component are eliminated.

4. Sample calculations

4.1 Application to a Fuel Assembly of a Prototype Fast Breeder Reactor

Fig.6 shows the schematic configuration of the calculation condition. A spiral wire is wrapped nine times, so that the number of the nodal plane is 55. The number of fuel pins in a subassembly is 169. The total number of elements is 39,655 (the beam element; 9,295, the joint element; 30,360). The total number of freedoms is 55,770.

Calculations were performed for two cases, the thermal bowing problems with and without wire effects.

Fig.7 shows the displacement profiles for the two cases in a nodal plane 52 (the axial distance of which is about 270cm from the lower fixed boundary). The solid circles show the pin positions after deformations, while broken circles show the initial positions. The

directions of the displacement of the pins are indicated by arrows. Fig.8 shows the lateral displacement profiles for the two cases in a row of pins along a line A-B shown in Fig.6. The solid lines show the pin positions after deformation, while broken lines show the initial positions. The signs, ↔, indicate the contact positions. From Fig.7 and Fig.8, the effect of wire tension is seen to affect significantly the equilibrium pin configurations.

4.2 Application to a 37 Pin Bundle during irradiation

To see the wire tension effect during irradiation, the irradiation bowing problems with and without wire effect were calculated for a fuel subassembly containing 37 fuel pins.

Fig.9 shows the schematic configuration of the calculation condition.

The computation started with normal configulation of fuel pins and followed 3 years' full power operation and then ended with power shut down. Blackburn equation /10/ was used for thermal creep and Gilbert equation /11/ for irradiation creep. The swelling equation for the fuel claddings and the spiral wires were HEDEL MARK 6 equation /12/ multiplied by 0.3, and 0.15, respectively in order to represent rather sever mechanical interaction between cladding and wire spacer, both of which are made of low swelling material.

Fig.10 shows the lateral displacement profiles for two cases in a row of pins along a line C-D shown in Fig.9.

From Fig.10, it is evident that the effect of wire tension is seen to affect significantly the equilibrium pin configurations.

5. Conclusion

A new model has been presented for the prediction of an equilibrium configuration of fuel pins in a fuel subassembly under steady state conditions in LMFBR cores.

A three-dimensional finite element code ÉTOILE has been programmed according to the newly developed model /13/ /14/. The code can simulate the mechanical properties in a cluster of up to 271 fuel pins during irradiation, taking into account the effects of spiral wire tension.

From sample calculations, it was confirmed that the present code is capable of a reasonable simulation of mechanical behaviours of fuel pins during irradiation. And, especially, it was shown that there are significant effects of wire tension on the fuel pin equilibrium configuration.

6. Acknowledgement

The author would like to express his grateful thanks to Mr. N. Shirakawa, Mr. T. Shimizu and Dr. K. Aoki of NAIG Research Laboratory, for their valuable discussions and sustained encouragement. He would also like to acknowledge Mr. T. Kobayashi and Mr. K. Okada of Toshiba Corporation, for providing the author with technological information for this study.

References

/1/ J. Rousseau et., "DEFORMATION DES AIGUILLES AVEC FIL ESPACEUR EN PRESENCE DE GONFILEMENT ET DE FLUAGE D'IRRADIATION", Irradiation behavior of Mechanical Materials for fast reactor Comporners, 1979, Corsica.

/2/ C. L. Dym, and I. H. Shames, "Solid Mechanics: A VARIATIONAL APPROACH", McGraw-Hill, 1973.

/3/ R. E. Goodman, R. L. Taylor, and T. Brekke, "A model for the mechanics of jointed rock", Proc. Am. Soc. Civ. Eng., 94, SM3, 637-59, 1968.

/4/ D. P. Chan, "DILATE - A 2-d structural program for the dilation response of hexagonal ducts", HEDL-TME 79-72 UC-79h, February 1980.

/5/ O. C. Zienkiewicz, "The Finite Element Method, 3rd ed.", McGraw-Hill, 1977.

/6/ R. S. Varga, "Matrix Iteration Analysis", Prentice-Hall, Inc., 1962.

/7/ C. MEYER, and A. C. SCORDELIS, "COMPUTER PROGRAM FOR PRISMATIC FOLDED PLATES WITH PLATE AND BEAM ELEMENTS", Structural Engineering and Structural Mechanics Report No.70-3, University of California, Berkeley, Feb. 1970.

/8/ C. L. Wheeler et., "COBRA-IV-I: An interim version of COBRA for thermal-hydraulic analysis of rod bundle nuclear fuel elements and cores", BNWL-1962 UC-32, March 1976.

/9/ R. H. Gallagher, "Finite element analysis: fundamentals", Prentice-Hall, Inc., 1975.

/10/ E. R. Gilbert, and L. D. Blackburn, "Creep deformation of 20 percent cold worked type 316 stainless steel", Journal of Engineering Materials and Technology, April 1977.

/11/ E. R. Gilbert, and J. F. Bates, "Dependence of irradiation creep on temperature and atom displacement in 20 percent cold worked type 316 stainless steel", Journal of Nuclear Materials vol.65, 204-209 (1977)

/12/ J. F. Bates, and M. K. Korenko, "Empirical development of irradiation induced swelling design equations", Nuclear Technology Vol.48, P.303, May, 1980.

/13/ Y. Kumaoka et., "LMFBR Core Design Based on Experimental Fast Breeder Reactor JOYO Experience", Toshiba Review No.140, July-Aug., 1982.

/14/ M. Nakagawa et., "ÉTOILE: A Three-dimensional Finite Element Code for the Analysis of Fuel Pin Deformations in an LMFBR Assembly", NAIG Annual Review, 1981.

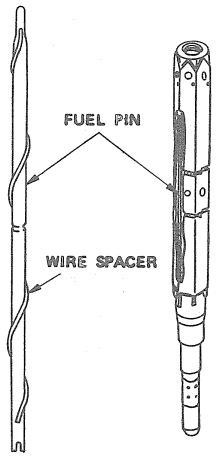

Fig. 1 Configuration of Fuel Pin with Wire Spacer and Fuel Subassembly

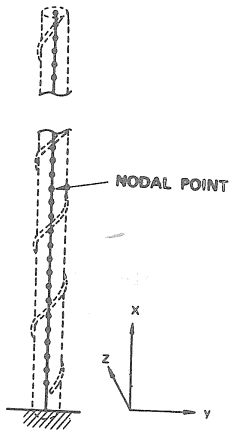

Fig. 2 Model of a Fuel Pin

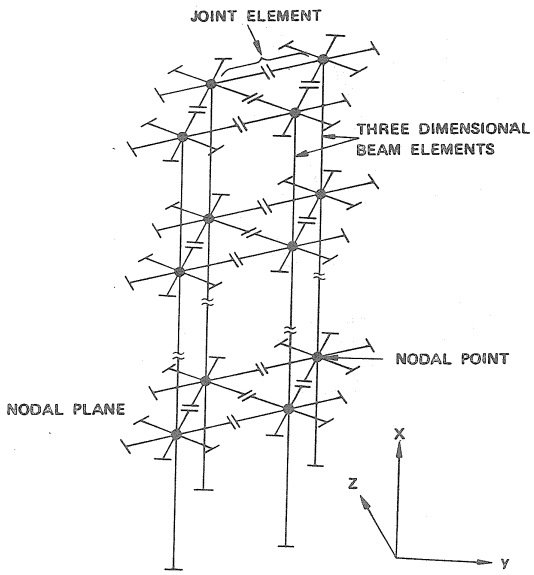

Fig. 3 Model of a Bundle of Fuel Pins

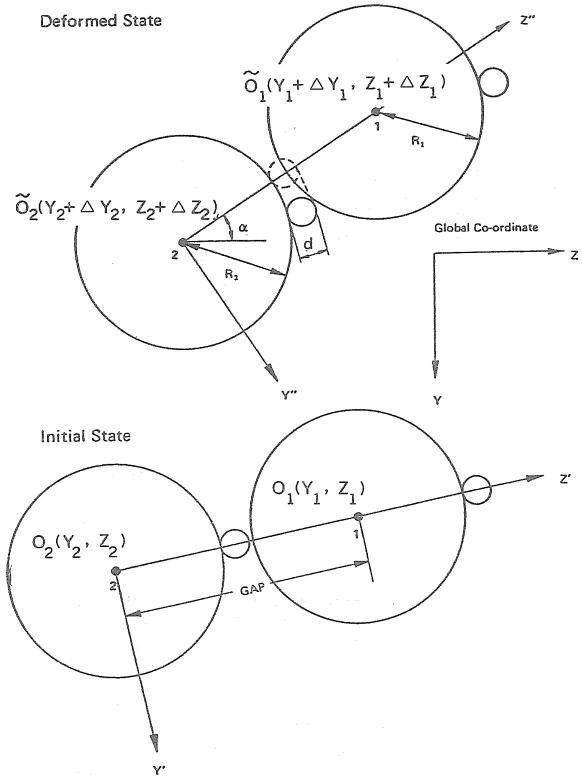

Fig. 4 Schematic Illustration of Contact Model

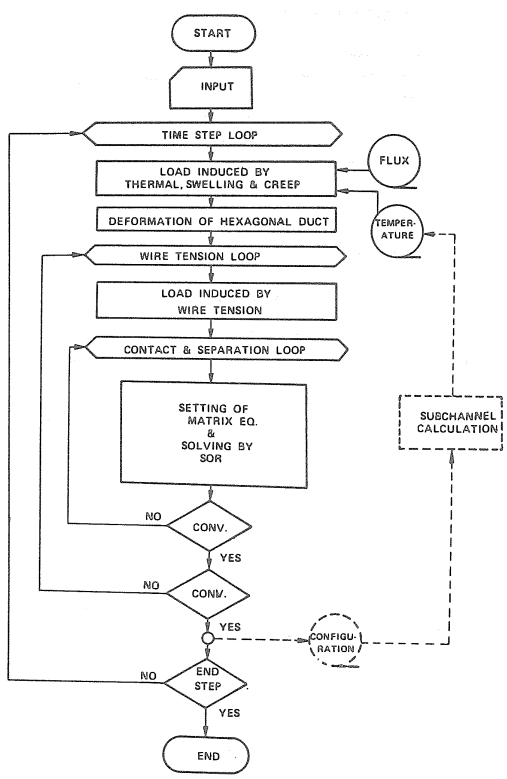

Fig. 5 Block Chart of ÉTOILE

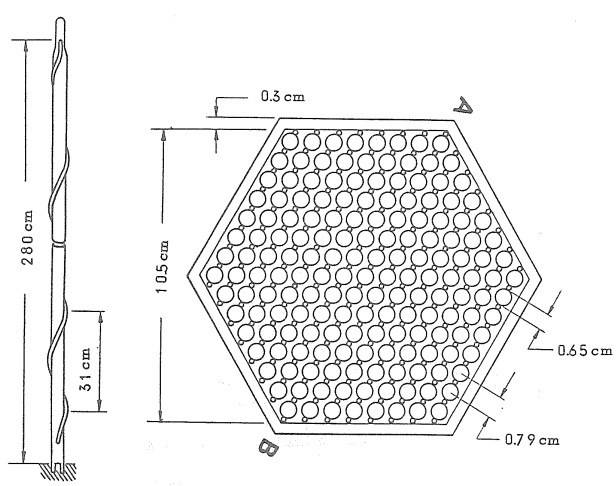

Fig. 6 Configuration of the Calculation Condition (Sec. 4.1)

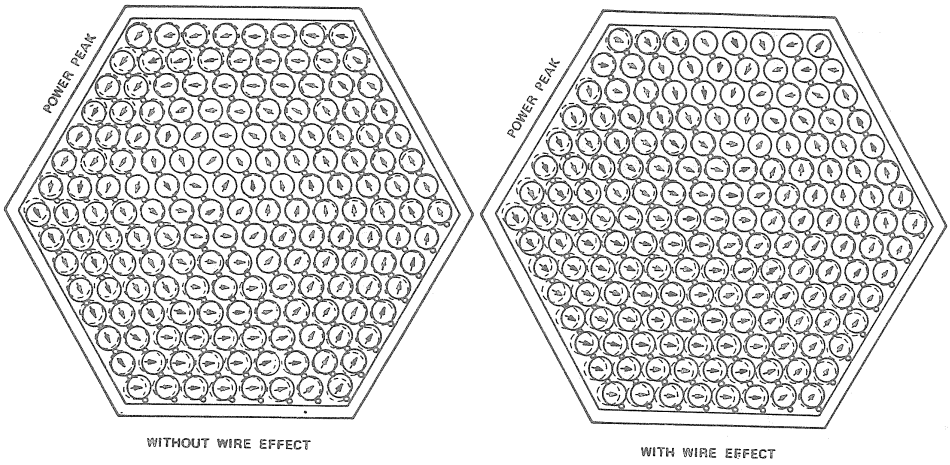

Fig. 7 Displacement Profile in a Nodal Plane 52

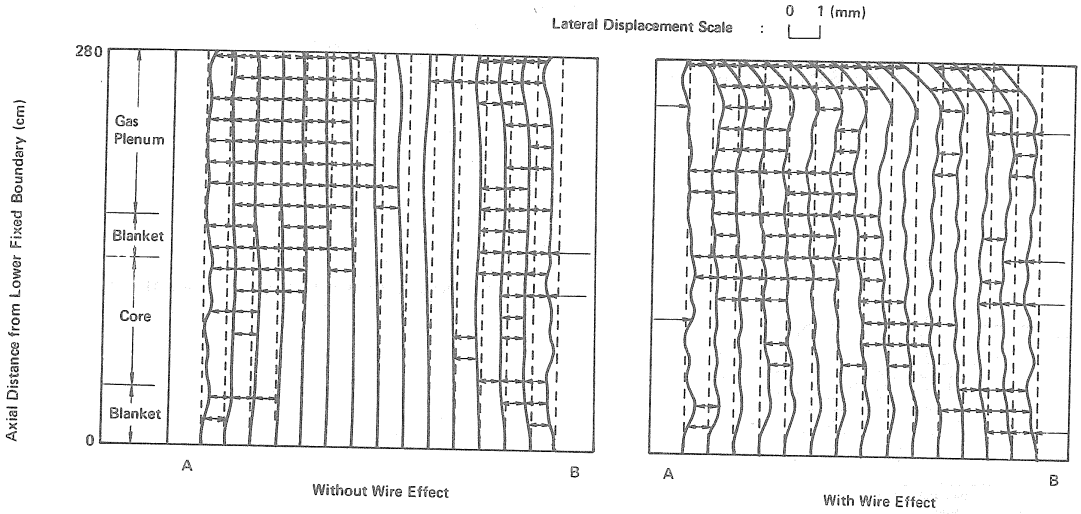

Fig. 8 Lateral Displacement Profile in a Row of Pins along a Line A–B Shown in Fig. 6

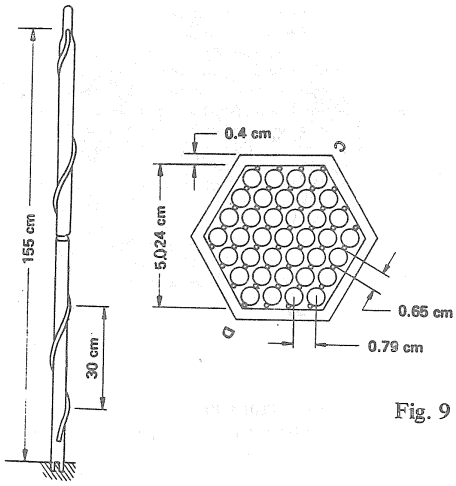

Fig. 9 Configulation of the Calculation Condition (Sec. 4.2)

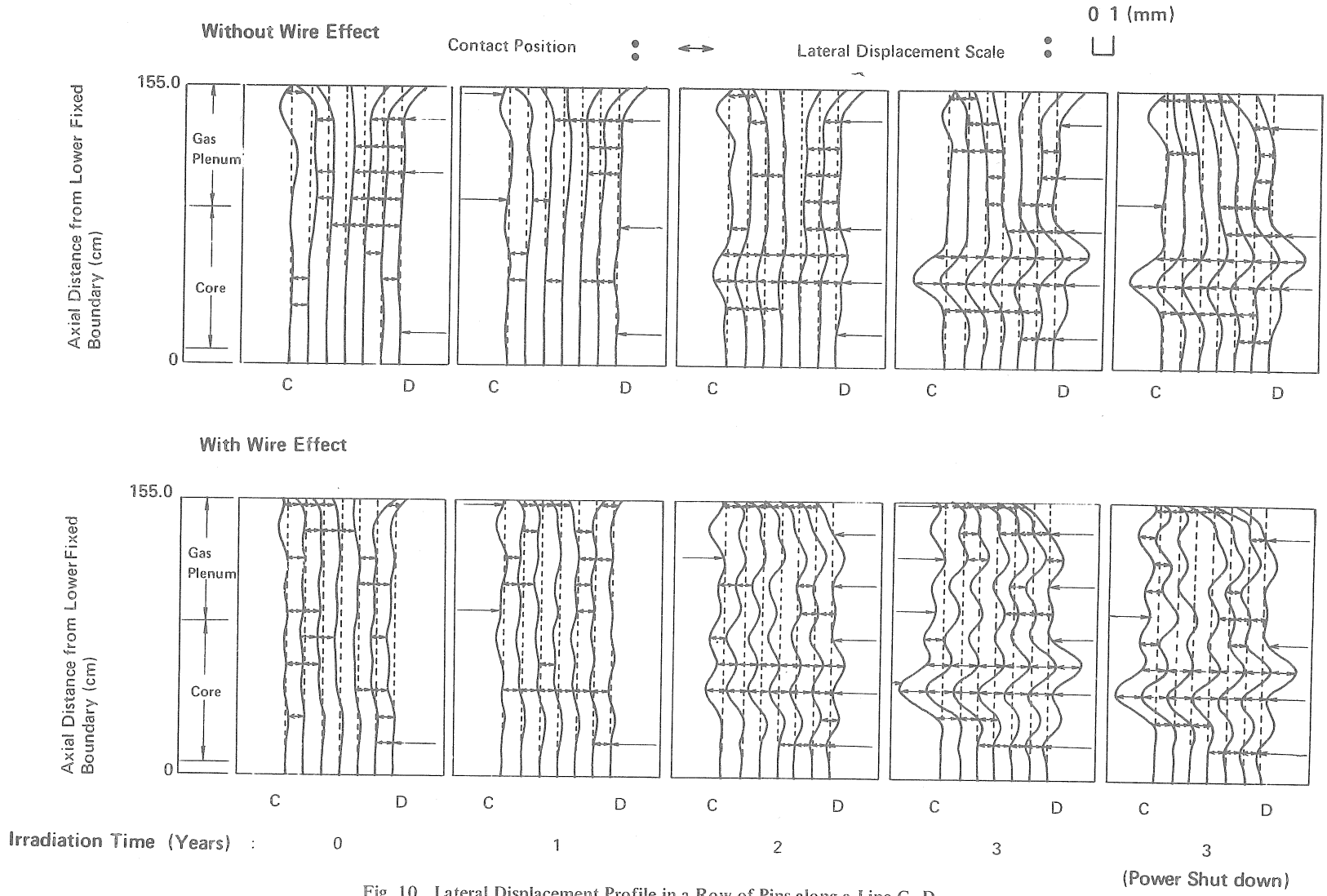

Fig. 10 Lateral Displacement Profile in a Row of Pins along a Line C–D Shown in Fig. 9